Ultrasonic Bonding of Membrane Electrode Assemblies for Low Temperature Proton Exchange Membrane Fuel Cells

Joseph Beck
Daniel Walczyk[1]
Casey Hoffman
Steve Buelte

Center for Automation Technologies and Systems, Rensselaer Polytechnic Institute, Troy, NY 12180

Low temperature proton exchange membrane (PEM) fuel cells currently dominate the fuel cell market, yet there are materials-, cost-, reliability-, and manufacturing-related challenges that hinder widespread commercial success of this promising technology. With regards to manufacturing, one of the main process bottlenecks is thermal bonding of electrode and membrane components into a unitized membrane electrode assembly (MEA). Recent work has shown that ultrasonic bonding can serve as a direct replacement for thermal bonding for high-temperature PEM fuel cells with dramatic reductions in cycle time and energy consumption but no significant degradation in performance. This paper investigates the possible use of ultrasonic bonding for low-temperature PEM MEAs operated at 65 °C. Polarization curves and 1000 Hz impedance were measured for MEAs with a five-layer architecture comprised of Nafion 115 membrane and carbon paper-based gas diffusion electrodes (GDE) that were thermally bonded and ultrasonically bonded using commercial equipment. The effect of membrane condition (conditioned and dry), electrode type (commercially available, custom-made with lower platinum loadings), and process conditions are investigated. Experimental results demonstrate clear trends. Both custom-made GDEs with lower platinum loading performed best suggesting that electrode architecture and composition can be optimized for ultrasonic bonding. There was little difference in performance between dry and conditioned membrane, which helps explain current industrial practice. Statistical analysis of an experimental design where ultrasonic bonding energy and pressure were varied suggests that neither parameter significantly affects MEA performance and that the process is robust. Similar analysis of thermal bonding with temperature and pressure varied suggests that temperature has a significant effect on MEA performance. However, the most important results of all experimentation are that process cycle time and energy consumption are reduced by nearly two orders-of-magnitude using ultrasonic bonding. [DOI: 10.1115/1.4007136]

1 Introduction and Background

Low-temperature proton exchange membrane (PEM) fuel cells currently dominate the fuel cell market [1]. Hence, there is significant interest in this growing industry to continually improve PEM cell performance, reliability, and robustness and also to reduce manufacturing costs. Improvements have been and will be made to materials, MEA and stack architecture, catalysts, bipolar plate designs, and production processes to reach these technical goals.

One new production process for PEM fuel cells (patent pending [2]) that is gaining significant attention is ultrasonic bonding of membrane electrode assemblies (MEAs), which is a direct replacement for traditional "hot" or thermal bonding. There is significant prior work described in the literature related to ultrasonic bonding of high-temperature PEM MEAs, particularly those made with PBI-based membranes (BASF Fuel Cell [3]), that has demonstrated order-of-magnitude reductions in process cycle time and energy consumption with no decrease in cell performance [4–7]. To date, however, no one has yet investigated whether ultrasonics can be applied to bonding of low-temperature PEM MEAs.

This paper investigates the potential of using ultrasonics to bond the components of five-layer low-temperature PEM MEAs and compares their performance to thermally bonded MEAs. MEAs consisting of Nafion membrane sandwiched between custom-made and commercial paper-based electrodes are tested in a single cell configuration. The effects that various process parameters have on MEA performance and optimal parameter values for both ultrasonic and thermal bonding are determined using designed experiments and statistical analysis. Additionally, the role that electrode type, catalyst loading, and membrane condition play in MEA performance is also assessed.

2 Materials and Experimental Methodology

2.1 Materials and Geometry. The membrane electrode assemblies (MEA) made for this experimental investigation are a standard five-layer architecture for low temperature PEM consisting of gas diffusion layer, catalyst layer (anode), membrane, catalyst layer (cathode), and gas diffusion layer. Catalyst ink is sprayed onto the gas diffusion layer coated with a microporous layer prior to thermal bonding or ultrasonic bonding, and this component is referred to as a gas diffusion electrode (GDE). An active area of 10.0 cm^2 was used for all fuel cell optimization and process parameter effects studies due to the availability of testing hardware and the authors' experience with this size. MEAs are made with GDE centered on an oversized membrane, as shown in Fig. 1, which also serves as a sealing surface for gaskets.

Three different GDEs were used to study the effect of electrode type on performance including a commercially available product from Fuel Cell Earth and two different types custom-made by the authors.

[1]Corresponding author.

Contributed by the Advanced Energy Systems Division of ASME for publication in the Journal of Fuel Cell Science and Technology. Manuscript received March 20, 2012; final manuscript received May 29, 2012; published online August 22, 2012. Editor: Nigel M. Sammes.

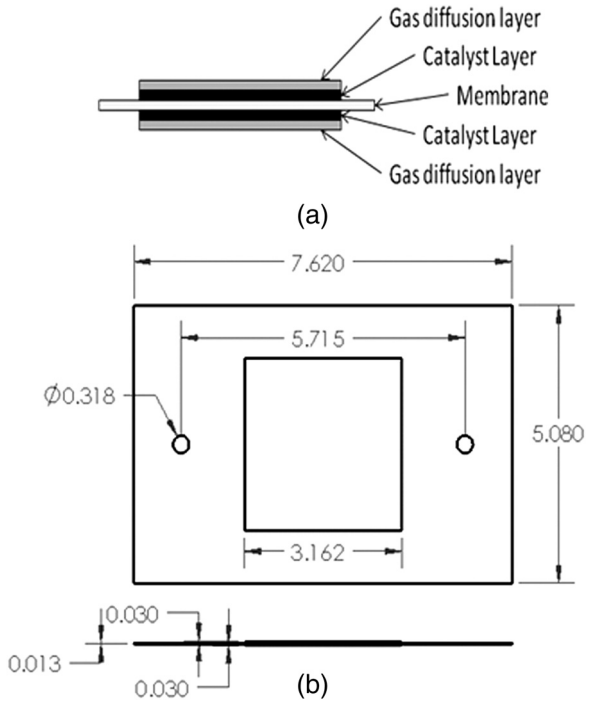

Fig. 1 (*a*) Schematic of standard 5-layer MEA architecture and (*b*) dimensioned (cm) drawing of low temperature MEA

The Fuel Cell Earth electrode model EP4019 is a 40% Pt on carbon, paper electrode with a reported loading of 0.5 mg Pt/cm^2 [8]. This electrode will be referred to as FCE.

The custom-made electrodes were produced by spray coating a catalyst layer on top of a commercially available gas diffusion layer (GDL) using a two-fluid, air-atomization, direct spray system (FCS200 Stainless Steel Spray Head from PVA, Cohoes, NY) on an electrode coating testbed designed by co-author Hoffman [9]. The GDLs used in this study were Sigracet SGL-25-BC, which already has a hydrophobic microporous layer [10]. The catalyst ink preparation (identical to that used by Hoffman [9]) was comprised of 20% platinum on Vulcan XC-72 Carbon, Nafion solution, isopropyl alcohol, and deionized water. The ratio of Nafion ionomer to carbon is 0.8:1 by weight. Multiple coats of this mixture were sprayed in thin layers and allowed to dry at room temperature until the desired platinum loadings of approximately 0.16 and 0.33 mg Pt/cm^2 were achieved, as measured by change in weight. These electrodes will be referred to as RPI Low and RPI High, respectively.

The membrane used, DuPont™ Nafion® N 115 [11], was cut by hand to 5.08 × 7.62 cm size using a scalpel and a template from an unconditioned roll of material. A portion of the MEAs tested during this research were conditioned in a process to hydrate and clean the membranes. Swelling of the Nafion membrane was observed during conditioning.

Conditioning of membranes involved a four step process used to remove impurities and hydrate the Nafion. Studies in the literature [12,13] show that preconditioning Nafion membranes improves ionic conductivity and performance (MEAs are usually thermal pressed in a sealed environment ensuring membrane hydration by preventing boil off). The cut membranes are first washed in boiling 3% hydrogen peroxide solution for 60 mins to oxidize organic impurities formed during the casting process. After allowing to cool to room temperature, they are then washed in boiling distilled water for 30 mins and again allowed to cool. To increase the degree of protonation of the membrane, the next step is a wash in boiling 0.5 M sulfuric acid for 60 mins. Finally, the membranes are washed in boiling water to remove any excess acid and allowed to cool before being rinsed with fresh distilled water. Distilled water is used throughout the conditioning process and the membranes are gently stirred repeatedly with a glass stirring rod to prevent them from curling out of the solution.

Once the membranes are fully conditioned, they are kept 100% hydrated prior to MEA bonding by submerging in distilled water in a large Pyrex dish. Dry, unconditioned membranes are stored in a ziplock bag to prevent changes in relative humidity. Measured thicknesses of the dry and fully hydrated, conditioned Nafion 115 membranes were 130 and 150 μm, respectively.

2.2 Ultrasonic Bonding. An ultrasonic bonding system, shown with components labeled in Fig. 2(*a*), consists of: a power supply, the ultrasonic stack consisting of a converter, booster, horn, and finally the anvil. The modified Branson 2000X Ultrasonic

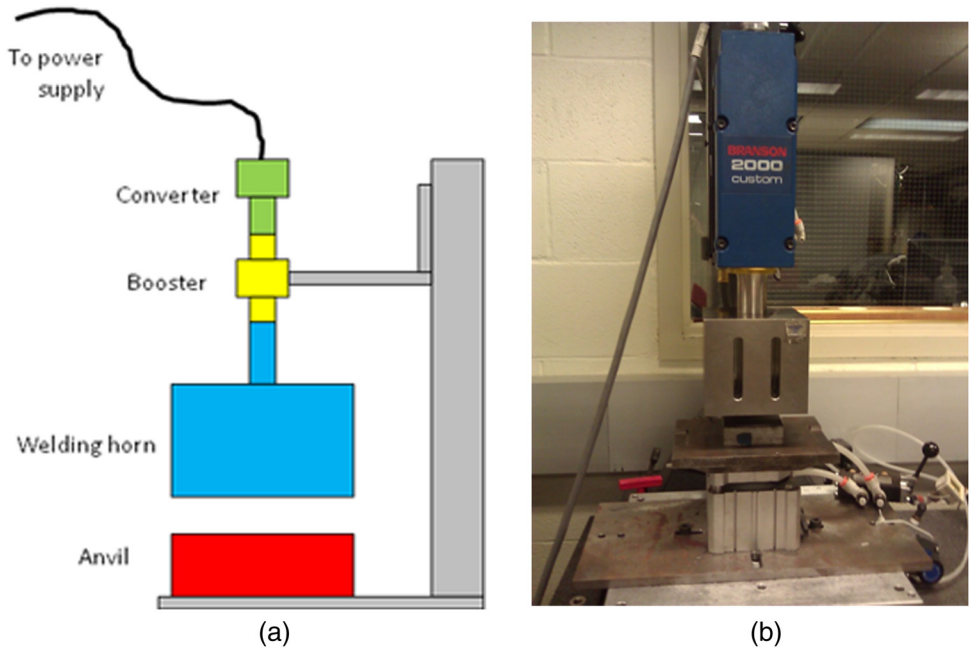

Fig. 2 (*a*) Labeled component diagram of ultrasonic bonding system and (*b*) actual system used for research

Bonding system used for this research is shown in Fig. 2(*b*). The power supply provides a 20 kHz waveform to the converter/transducer which converts the electrical energy into a mechanical oscillation of the same frequency using a piezoelectric device. Increasing or decreasing the amplitude of the oscillation is achieved by a mechanical advantage in the booster. Connected to the booster is the ultrasonic welding horn designed for constant vibrational amplitude at the surface of the horn. The anvil is the nonvibrating base of the system, where the MEA components are assembled prior to sealing.

The Branson system shown in Fig. 2(*b*) can apply a maximum load of about 4.5 kN, which translates to 4.5 MPa of sealing pressure acting over the 10 cm^2 active area. Raising a pneumatic cylinder from below applies a specified preload force to the MEA components prior to sealing. The anvil mounted to the cylinder is pressed up into the horn while the MEA components are sandwiched in between. Sealing pressure is controlled by varying the air pressure supplied to an air cylinder.

The ultrasonic bonding system can run on various welding control modes based on energy, time, or displacement. The amount of energy applied is a function of time, pressure, amplitude, and frequency. All MEAs were bonded using the *controlled energy mode*, where the power module supplies a fixed amount of energy to the ultrasonic stack. It should be noted that not all of the electrical input energy is used in bonding the materials together due to small losses through the system including, but not limited to anvil vibration (internal damping) and noise [4].

The anvil used in manufacturing the MEAs was 7.6 cm square, and the welding surface was ground flat and parallel. The 20 kHz tuned ultrasonic horns, manufactured by Branson, measured 12.7 cm square, had either knurled or smooth surfaces, and attached to the transducer using either a 1:1 or 1:1.5 booster. In the latter case, the $\pm 10\,\mu$m vibrational amplitude from the converter was increased to $\pm 15\,\mu$m using the 1.5 × booster. The fine, female knurl on the horn face had a spacing of about 0.5 mm and groove depth of approximately 0.25 millimeters.

MEA components are assembled carefully by hand to ensure alignment. An electrode is placed catalyst side up on a large piece of Kapton. Immediately prior to sealing, the membrane is removed from the distilled water bath and any excess water on the surface is removed using a paper towel. This accommodates for the potential change in membrane dimensions, which can be up to 15%, due to the sensitivity of Nafion to relative humidity [11]. The membrane is carefully placed above first electrode followed by the second electrode with active area facing down making certain that the electrodes are aligned with each other and centered on the Nafion. A second piece of Kapton is placed over the assembly and gently pressed down to prevent the MEA architecture from shifting. The Kapton allows the user to easily transport and place the MEA on the anvil for ultrasonic sealing. A diagram of the hand-assembled MEA components is shown in Fig. 3.

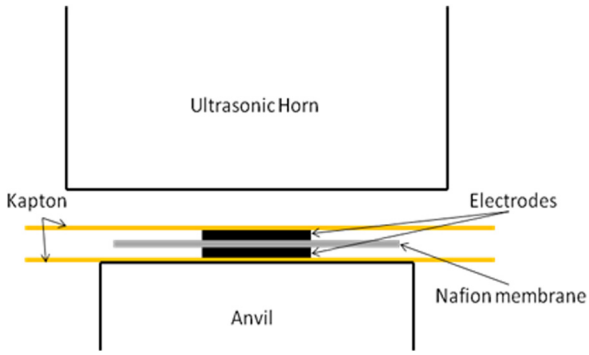

Fig. 3 Schematic of labeled MEA made by hand in ultrasonic setup prior to bonding

Once an MEA is centered on the anvil, the load is applied by raising the anvil to the face of the horn. Figure 3 shows MEA components in the ultrasonic setup prior to the ultrasonic bonding process. The ultrasonic welding continues until the prescribed energy level has been reached. Following ultrasonic sealing, the anvil is lowered and the MEA is stored in sealable polyethylene bags until it is tested. Ultrasonically bonded MEAs with hydrated membranes are stored in a paper towel dampened with distilled water inside the bag to prevent them from dehydrating. A lack of hydration during storage causes the MEA to curl and shrivel up thereby preventing assembly. MEAs made with dry membrane are stored without additional hydration.

2.3 Thermal Bonding. A 40-ton hot press built by Progressive Machine and Design (Victory, NY) was used to thermally bond MEAs (Fig. 4(*a*)). The upper and lower platens are ground flat and can be independently temperature controlled during the sealing process. The load capacity is measured with an in-line load cell and controlled using servo valves for the hydraulic ram and a PID loop for pressure control.

The thermal press was used to control the temperature and pressure during the thermal bonding of MEAs. The platen temperature was allowed to reach steady state before bonding. All MEAs used for this research were thermally pressed with a high durometer rubber compliance layer (3.2 mm thick piece of urethane) placed on top of the lower platen with a thin Kapton layer in between to prevent sticking. The rubber layer, which helped to even out pressure applied to the MEA, was allowed to heat up to temperature with the press prior to MEA bonding. The same MEA and Kapton layers used for ultrasonic bonding were placed in the middle of the lower rubber layer, as shown in Fig. 4(*b*).

The MEA components are placed on the lower platen and the bonding cycle is started as soon as possible, typically within 2–3 seconds. Press operation for sealing an MEA involves the

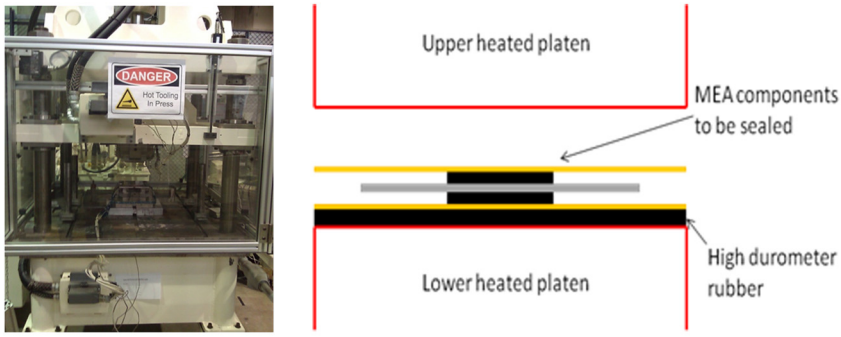

Fig. 4 (*a*) 40 ton hot press used to bond MEAs and (*b*) schematic of MEA in press prior to thermal sealing

upper platen rapidly descending at about 1 cm/sec to 5 mm above the surface of the MEA then creeping downward at about 1 mm/sec until the desired load is reached and held for the prescribed hold time. Elapsed time from MEA placement to when the upper platen first contacts the MEA components is approximately 5 sec. After the press holds at pressure for the set time (120 sec), the upper platen creeps back up to slightly above the MEA and then rapidly moves to its home position. At this point, the MEA is quickly removed from the lower platen and placed on a table top to cool to room temperature. The thermally bonded MEA was removed by peeling off the Kapton and placing it in a polyethylene bag prior to testing.

2.4 Testing Procedure and Protocol. After alignment holes are punched on the MEA membrane using a jig and precision round punch, individual MEAs are clamped into the cell hardware, shown in Fig. 5, consisting of two stainless steel end plates with integrated heaters, gold plated current collectors, and anode and cathode flow field plates. A single channel serpentine geometry was machined on the gas flow field plates. Perfluoroalkoxy (PFA) gaskets are used to control MEA compression within the cell hardware to approximately 20%. Gasket thickness is based on the relationship $T_{gasket} = 0.8*(T_{MEA} - T_{membrane})/2$, where T_{MEA} is the MEA thickness and $T_{membrane}$ is the membrane thickness.

MEA performance was tested using a Fuel Cell Technologies test stand equipped with a AMREL (American Reliance, Inc.) PLA800-60-300UL load bank capable of drawing up to 300 A current. Hydrogen or nitrogen gas can be supplied to the anode side, and oxygen, air, or nitrogen can be supplied to the cathode side of the cell. The test station incorporated humidifiation for the anode and cathode gasses and heated gas supply tubes to prevent condensation between the humidifier and the cell. Mass flow controllers independently control the mass gas flow on both the anode and cathode. Once the gasses have passed through the cell, they are safely vented to the exhaust system. The test stand also includes a temperature controller with heaters to control the operating temperature of the cell.

A LABVIEW program interface controls the fuel cell testing procedure automatically. Polarization curves for both H_2/O_2 and H_2/Air were collected by the test stand computer to help characterize the performance of each MEA.

The standard testing procedure for MEAs tested in this research includes a period of time for the cell and test hardware to reach steady-state operating conditions, a burn in period at high current density, steps to oxidize and reduce any species on the cathode, H_2/O_2 polarization curve, H_2/Air curve, and finally a cool down.

Cell operating temperature during the test procedure is 65 °C, and the cell is maintained at temperature using the cartridge heaters integrated into the endplates. The anode and cathode gas humidifiers were maintained at 61 °C. Throughout testing the anode and cathode stoichiometry was maintained at 2.0. All MEAs were tested at atmospheric pressure.

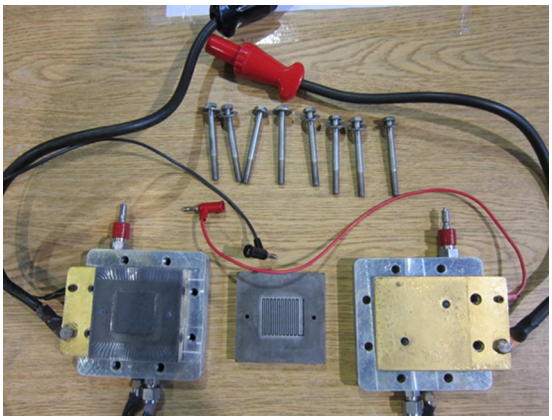

Fig. 5 Cell testing hardware

3 Effect of Electrode Type on MEA Performance

To test the effect of electrode loading and architecture on the performance of the thermal and ultrasonic bonding processes, MEAs were pressed with three different electrodes as described previously in Sec. 2.1: FCE, RPI Low and RPI High. The ultrasonic sealing parameters used were 8.0 Js/mm^2 energy flux (i.e., 8000 J energy ÷ 1000 mm^2 active area) and 4.4 N/mm^2 pressure. Energy flux in J/mm^2 is defined as the total energy the ultrasonic power supply provides to the stack divided by the active area of the MEA. Sealing pressure (N/mm^2 or MPa) is the total force applied by the ultrasonic welding system divided by the active area. MEAs were thermally bonded at 150 °C, 2.0 N/mm^2 sealing pressure, and held for 120 seconds, while an 80 durometer (Shore A) urethane layer underneath the anvil provided some compliance. All membranes were conditioned Nafion 115. Performance was measured using polarization curves run with H_2/O_2 at 2.0 stoichiometric ratios. A fixed stoichiometric ratio was selected that was common in the literature [14,15] for fuel cell testing of non-flow-related effects. Figures 6 and 7 show performance of the three ultrasonically bonded and three thermally bonded MEAs, respectively.

Both custom sprayed GDEs (RPI High and Low) with lower catalyst loading outperformed the commercial GDE (FCE) in the ultrasonically bonded MEAs. The RPI Low electrode performance was 69 and 114 mV higher at 0.6 and 0.8 A/cm^2, respectively, as compared to the FCE. Similarly, the RPI High electrode performance was 142 and 217 mV higher at 0.6 and 0.8 A/cm^2, respectively, as compared to FCE. As expected, the higher loaded RPI electrode had better performance than the lower loaded RPI electrode due to the increased number of reaction sites. If the same performance can be achieved using GDE with a lower catalyst loading, significant material cost savings can be realized.

The custom GDEs (RPI High and Low) with lower catalyst loading outperformed the commercial electrodes (FCE) in

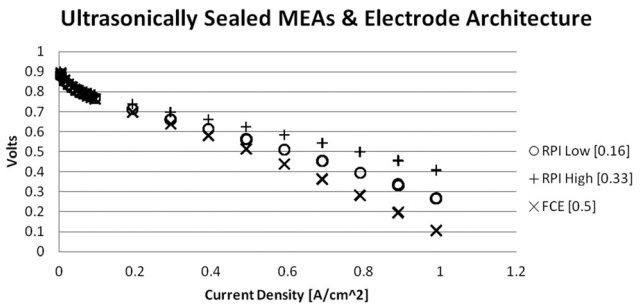

Fig. 6 Effect of electrode loading and architecture on ultrasonically bonded MEAs

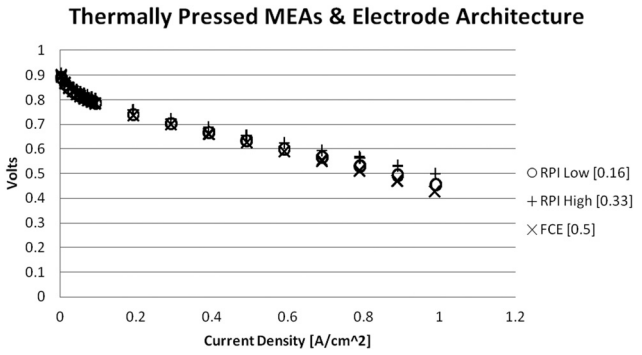

Fig. 7 Effect of electrode loading and architecture on thermally bonded MEAs

ultrasonically bonded MEAs. As expected, the higher loaded RPI electrode had better performance than the lower loaded RPI electrode due to the increased number of reaction sites. If the same performance can be achieved using GDE with a lower catalyst loading, significant material cost savings can be realized.

The effect of electrode type on performance for ultrasonically bonded MEAs suggests that electrode architecture is very important for ultrasonic bonding of low temperature MEAs. The vibrations from the ultrasonic process may affect certain GDLs more than others. Possible effects include: (1) breaking fibers in the GDL which would decreases electrode conductivity, or (2) closing pores in the microporous layer which would increase gas diffusion resistance and hurt cell performance. Optimizing the catalyst ink composition for ultrasonic bonding may improve the bond between the electrode and Nafion membrane.

Thermally pressed MEAs with the various electrodes exhibited the same relative performance trends as the ultrasonically bonded versions, but variance between the three MEA performances is much smaller. At 0.8 A/cm^2, the difference between the RPI High and the FCE is about 50 mV, while the difference is over 200 mV for the same ultrasonically bonded MEAs. Presumably, resulting MEA performance using the ultrasonically bonding process is more sensitive to electrode architecture than the standard thermal pressing process, which would be expected. Current commercial GDEs have been optimized through extensive research and development efforts for thermal pressing of MEAs.

Performance in the activation region for both manufacturing processes is very similar across all MEAs. Ultrasonically bonded MEAs in this study had larger ohmic region losses indicating an increased cell resistance. The ultrasonically bonded MEAs exhibited an approximate 25 mΩ increase in 1000 Hz impedance at room temperature compared to the thermally bonded MEAs.

4 Effect of Membrane Conditioning on MEA Performance

As previously mentioned, the fuel cell industry typically uses low-temperature membrane as supplied by the manufacturer for MEA production, while many researchers condition/hydrate the membrane beforehand to improve performance but at the expense of ease of manufacturing. To investigate the effect of membrane conditioning, MEAs were thermally and ultrasonically pressed with RPI Low, RPI High, and FCE electrodes using the Nafion 115 membrane in both conditions, as described in Sec. 2.1. Thermal press process parameters were fixed at 150 °C, 2.0 N/mm^2, 120 seconds hold time, and 80 Shore A durometer rubber compliance layer. Ultrasonic MEAs were bonded with energy flux of 8.0 J/mm^2 and 4.4 N/mm^2 of sealing pressure. Performance data was collected from polarization curves with cells running H_2/O_2 with 2.0 stoichiometric ratios and 1 atm gas pressure. All testing results are from short term testing only; approximately six hours per test which includes a 90 min burn-in step.

Performance voltage data at 0.4, 0.6, and 0.8 A/cm^2 current densities for the different electrode types and bonding processes is shown in Table 1. "Cond." represents MEAs that were bonded with conditioned membranes and "Dry" refers to unconditioned membranes.

Performance for ultrasonically bonded MEAs improved to varying degrees when using unconditioned membrane with all electrodes. The most dramatic improvements were with FCE and RPI Low electrodes, and only slight improvement is observed with RPI High electrode. This improvement is likely due to the improved bonding between electrodes and the dry membrane. Some percentage of the ultrasonic energy goes into heating the water in the hydrated, conditioned membrane, so less energy is then available to bond the MEA components together, thereby resulting in higher cell resistance and greater losses.

As compared to conditioned membranes, there was a slight decrease in performance when dry, unconditioned membranes were used in thermally pressed MEAs for both RPI High and RPI Low membranes. Conditioning membranes improves the membrane ionic conductivity by ensuring complete protonation and increased water content. Hence, one would expect significant improvements in MEA performance using conditioned membranes. However, MEAs with conditioned membranes are usually hot pressed in hermetically sealed bags to prevent dehydration, and the overall bonding operation is usually much longer than the 120 seconds used here. The extra step of hermetically sealing the MEA and longer cycle time are not conducive to a production process, which probably explains why industry chooses to use dry membrane instead. With the absorbed water in the conditioned membrane able to easily boil off in the open thermal bonding shown in Fig. 4, it is no surprise that both dry and conditioned membranes in thermally bonded MEAs have similar performance.

Table 1 Performance results for membrane conditioning testing at three current densities over both thermal and ultrasonic MEA bonding

Manufacturing process and parameters		Voltages		
		0.4 A/cm^2	0.6 A/cm^2	0.8 A/cm^2
RPI Low (0.16)	Cond. ultrasonic	0.615	0.512	0.398
	Dry ultrasonic	0.646	0.564	0.474
	Cond. thermal	0.666	0.598	0.530
	Dry thermal	0.661	0.593	0.522
RPI High (0.33)	Cond. ultrasonic	0.663	0.584	0.501
	Dry ultrasonic	0.672	0.595	0.512
	Cond. thermal	0.686	0.623	0.562
	Dry thermal	0.679	0.610	0.539
FCE (0.5)	Cond. ultrasonic	0.581	0.443	0.284
	Dry ultrasonic	0.659	0.581	0.494
	Cond. thermal	0.661	0.588	0.511
	Dry thermal	0.663	0.592	0.517

The commercial electrode showed improved performance under both ultrasonic and thermally bonded conditions using unconditioned membrane. Thermally bonded MEAs had very small differences between the membrane conditions, less than 10 mV at all current densities. Ultrasonics and commercial electrode showed the greatest improvement with the dry membrane of 78, 139, and 210 mV at 0.4, 0.6. and 0.8 A/cm^2, respectively.

5 Thermal Bonding Optimization and Energy Consumption

The objective of the thermal bonding optimization study was to optimize sealing temperature and pressure. Bonding hold time was held constant in this study, because Liang et al. [16] concludes that as long as the MEA is pressed long enough to not delaminate, bonding time has little or no effect on performance. Therefore, sealing temperature and pressure were the only factors in the optimization. Temperature is recorded in °C and sealing pressure in the press is measured in N/mm^2. All MEAs for this thermal bonding study consisted of FCE electrodes and conditioned Nafion membranes.

The DOE used in this case was a randomized complete block design involving three levels for two factors. MEAs were pressed with 2, 4, and 8 N/mm^2 sealing pressures and 130, 150, and 170 °C sealing temperatures. Bonding time was held constant at 120 seconds as well as an 80 durometer Shore A compliance layer. The previously described procedure to randomize selection and assignment of the electrodes and testing of the MEAs was applied. Due to the limited size of the electrode sheets, the experiment had to be divided into two blocks of electrode material. Two sheets of GDE were required to supply enough electrodes for all MEAs. One replicate of each combination of manufacturing parameters was tested in each block which resulted in two replicates total.

Table 2 Thermal performance data for ANOVA

Pressure (N/mm^2)	Temperature (°C)	Electrode	Voltage @ 0.4 A/cm^2, O_2	Voltage @ 0.6 A/cm^2, O_2	Voltage @ 0.8 A/cm^2, O_2	Voltage @ 0.4 A/cm^2, air	Voltage @ 0.6 A/cm^2, air	Voltage @ 0.8 A/cm^2, air
2	130	A	0.647	0.560	0.455	0.575	0.426	0
2	130	B	0.653	0.568	0.473	0.581	0.431	0.081
2	150	A	0.663	0.588	0.509	0.595	0.463	0.157
2	150	B	0.671	0.600	0.524	0.597	0.477	0.227
2	170	A	0.687	0.629	0.571	0.611	0.520	0.368
2	170	B	0.682	0.624	0.565	0.611	0.510	0.297
4	130	A	0.651	0.567	0.467	0.576	0.417	0
4	130	B	0.638	0.525	0.382	0.580	0.373	0
4	150	A	0.671	0.601	0.526	0.596	0.476	0.253
4	150	B	0.678	0.612	0.543	0.608	0.44	0
4	170	A	0.685	0.624	0.564	0.607	0.476	0.153
4	170	B	0.685	0.625	0.568	0.607	0.493	0.241
8	130	A	0.631	0.546	0.440	0.562	0.418	0.095
8	130	B	0.636	0.543	0.433	0	0	0
8	150	A	0.663	0.590	0.51	0.589	0.454	0.255
8	150	B	0.670	0.590	0.503	0.600	0.401	0
8	170	A	0.677	0.606	0.530	0.596	0.479	0.242
8	170	B	0.640	0.546	0.442	0.551	0.425	0.164

Table 3 Two-way ANOVA table for thermal optimization at 0.4 A/cm^2 and O_2 on the cathode

Analysis of variance table					
Response: O2_V4	Df	Sum sq	Mean sq	F value	Pr(>F)
Temperature	2	0.0037333	0.00186667	17.2418	0.001257**
Pressure	2	0.0008723	0.00043617	4.0287	0.061610
Electrode	1	0.0000269	0.00002689	0.2484	0.631640
Temperature: pressure	4	0.0004093	0.00010233	0.9452	0.485617
Residuals	8	0.0008661	0.00010826		

Table 4 Two-way ANOVA table for thermal optimization at 0.6 A/cm^2 and O_2 on the cathode

Analysis of variance table					
Response: O2_V6	Df	Sum sq	Mean sq	F value	Pr(>F)
Temperature	2	0.0110188	0.0055094	17.4486	0.00121**
Pressure	2	0.0022121	0.0011061	3.5029	0.08078
Electrode	1	0.0003380	0.0003380	1.0705	0.33110
Temperature: pressure	4	0.0018262	0.0004566	1.4459	0.30393
Residuals	8	0.0025260	0.0003157		

Table 5 Two-way ANOVA table for thermal optimization at 0.8 A/cm^2 and O_2 on the cathode

Analysis of variance table					
Response: O2_V8	Df	Sum sq	Mean sq	F value	Pr(>F)
Temperature	2	0.032219	0.0161097	18.6641	0.0009703***
Pressure	2	0.005344	0.0026721	3.0957	0.1009831
Electrode	1	0.001073	0.0010734	1.2436	0.2971566
Temperature: pressure	4	0.005854	0.0014634	1.6954	0.2432425
Residuals	8	0.006905	0.0008631		

Multiple GDE material sheets used are a nuisance factor and the blocking allows for more precise conclusions by removing the variation in performance by the blocked factor from the error term in the ANOVA.

Similar to the ultrasonic optimization, main and interaction effects were estimated using ANOVA on performance of the MEA at three different current densities. Performance data was parsed out from H_2/O_2 and H_2/Air polarization curves. One-way and two-way ANOVAs tested for main effects. Table 2 shows performance data used in thermal ANOVA.

The two-way (temperature * sealing pressure) ANOVA for H_2/O_2 MEA performance at 0.4 A/cm^2, shown in Table 3, reveals that MEA performance was significantly different across the bonding temperature conditions ($P < 0.01$) resulting in a main effect of temperature, while also suggesting no sealing pressure main effect. No interaction effect between pressure and temperature is suggested. Note that the blocked electrode factor had no statistically significant effect on the performance. One-way ANOVA estimates temperature to be a main effect ($P < 0.001$), while bonding pressure to have no effect on the performance.

The two-way (temperature * sealing pressure) analysis of variance table of H_2/O_2 MEA performance at 0.6 A/cm^2, shown in Table 4, suggests that the variance in performance can be explained by the variation in temperature during the manufacturing process ($P < 0.01$). Pressure is estimated to not be a main effect as well as no interaction effect. The main effect conclusions do not change when completing a one-way ANOVA on temperature and pressure individually.

Similar to the lower current densities, the two-way (temperature * sealing pressure) analysis of variance table of H_2/O_2 MEA performance at 0.8 A/cm^2, shown in Table 5, estimates temperature to be a main effect ($P < 0.001$), no main effect of sealing pressure ($P > 0.05$), and no interaction effect ($P > 0.05$). One-way ANOVA revealed performance is significantly different across the three bonding temperatures ($P < 0.001$). Pressure is not a main effect when tested in a one-way ANOVA.

Thermal bonding parameters of 170 °C and 2.0 N/mm^2 during the standard 120 s cycle time produced the highest performance in MEA polarization curves, and performance improved with increasing bonding temperature. Higher manufacturing temperatures resulted in slightly thinner final MEAs with increased bonding between the electrodes and membrane. Better contact between the components reduces the cell resistance thereby improving the MEA performance. These results are similar to Zhang [17], that is, MEAs pressed at a higher temperature exhibit improved performance.

Power versus time data was collected during thermal bonding of MEAs using optimal process conditions (i.e., 170 °C, 2.0 N/mm^2, 120 s). To account for all the energy required to run the thermal press, current and voltage measurements were taken upstream, i.e.,

at the press's electrical power cord, using Flex-Core Model CTI-150 current transformers connected to a WattsOn™ Universal Power Transducer in conjunction with WattsOn Console Software [18]. Data recorded during press warm up, "stand-by" state, bonding cycles, and cool down helped decompose the total energy consumption into the different contributions.

Four MEAs were thermally pressed while real and reactive power data was recorded. Real power is the electrical power that does actual work on the load and what the user pays the electrical utility for. The average bonding cycle on the thermal press requires 5.40 kW during operation. Multiplying this average power by time (120 second bonding cycle) yields an average energy consumption of 0.18 kWh (0.648 MJ) needed to thermally press one MEA.

6 Ultrasonic Bonding Optimization and Energy Consumption

Energy flux and sealing pressure, the two important manufacturing variables in the ultrasonic bonding process, were optimized through a design of experiments (DOE). A full factorial, completely randomized experiment with two replicates was completed to estimate the effects of each manufacturing parameter on MEA performance. FCE electrodes and conditioned Nafion membranes were used for this study.

A prescreening experiment was conducted prior to the optimization study to determine the levels of the manufacturing factors. The final experiment tested $(3 \times 2) \times 2$ replicates $= 12$ MEAs made with energy flux levels of 3.0, 6.0, and 9.0 J/mm^2, and sealing pressure levels of 3.0 and 4.5 N/mm^2. Electrodes for each MEA were cut from a larger sheet and given a unique identification number. Two electrodes were then paired randomly for bonding into a single MEA, each electrode pair was randomly assigned to a combination of manufacturing factors and levels, and finally MEAs were manufactured and tested in random order. This testing approach minimizes the effect on the response variable by any nuisance variables

Main and interaction effects were estimated using Analysis of Variance (ANOVA) on performance of the MEA at three different current densities. The voltages for each data point were averaged from the H_2/O_2 polarization curves at each specified current density. Three separate ANOVAs tested for main effects. Ultrasonic MEA performance data used for main effect estimation is shown in Table 6.

The two-way (energy flux * sealing pressure) ANOVA results of MEA performance at 0.4 A/cm^2 including p-values for each factor is shown in Table 7. A two-way ANOVA suggests no main effect (i.e., $p > 0.05$) for energy flux and sealing pressure, and no interaction effect between them. The p-values from the analysis are above the 95% confidence level probability, where the null hypothesis would be rejected in favor of the alternate hypothesis stating that the variance in performance can be explained by variation in the tested factor. While the interaction effect between energy flux and pressure is the most significant in this data set, it is not statistically significant enough to explain the variance in the response variable. One-way ANOVAs on the factors individually did not yield any different main effect estimates.

Table 6 Ultrasonic performance data for ANOVA with H_2/O_2

Energy flux (J/mm^2)	Pressure (N/mm^2)	Voltage @ 0.4 A/cm^2	Voltage @ 0.6 A/cm^2	Voltage @ 0.8 A/cm^2
9	3	0.644	0.553	0.439
3	4.5	0.621	0.506	0.344
9	3	0.632	0.522	0.382
9	4.5	0.588	0.437	0.231
6	4.5	0.627	0.503	0.343
6	4.5	0.597	0.422	0.144
6	3	0.614	0.457	0.248
3	4.5	0.624	0.482	0.246
3	3	0.578	0.345	0.027
9	4.5	0.542	0.329	0.079
3	3	0.628	0.511	0.344
6	3	0.635	0.517	0.357

Table 7 ANOVA table for ultrasonic optimization at 0.4 A/cm^2

Analysis of variance table

Response: O2_V4	Df	Sum sq	Mean sq	F value	Pr(>F)
Energy	2	0.0005832	0.00029158	0.5727	0.59209
Pressure	1	0.0014520	0.00145200	2.8517	0.14224
Energy: pressure	2	0.0044135	0.00220675	4.3340	0.06844
Residuals	6	0.0030550	0.00050917		

Table 8 Two-way ANOVA table for ultrasonic optimization at 0.6 A/cm^2

Analysis of variance table

Response: O2_V6	Df	Sum sq	Mean sq	F value	Pr(>F)
Energy	2	0.0005332	0.0002666	0.0628	0.9397
Pressure	1	0.0042563	0.0042563	1.0031	0.3552
Energy: pressure	2	0.0245702	0.0122851	2.8953	0.1318
Residuals	6	0.0254590	0.0042432		

Table 9 Two-way ANOVA table for ultrasonic optimization at 0.8 A/cm^2

Analysis of variance table

Response: O2_V8	Df	Sum sq	Mean sq	F value	Pr(>F)
Energy	2	0.003965	0.001983	0.1266	0.8834
Pressure	1	0.014008	0.014008	0.8945	0.3808
Energy: pressure	2	0.066743	0.033372	2.1309	0.1999
Residuals	6	0.093964	0.015661		

The two-way (energy flux * sealing pressure) ANOVA output for MEA performance at 0.6 A/cm^2 including p-values for each factor is shown in Table 8. A two-way ANOVA of voltages at 0.6 A/cm^2 estimates that performance voltage was not statistically significant across the three energy flux levels. Variation in sealing pressure did not explain the variation in the voltage, and no interaction effect existed. P-values from one-way ANOVAs are all greater than 0.05.

The two-way (energy flux * sealing pressure) ANOVA output for MEA performance at 0.8 A/cm^2 including p-values for each factor is shown in Table 9. A two-way ANOVA suggests no main effect of energy or pressure and no interaction effect. The variation in the performance data at 0.8 A/cm^2 cannot be explained by the variation in either of the manufacturing factors.

No main effects of energy flux or sealing pressure are estimated from the ultrasonic optimization study. This suggests that the ultrasonic bonding process is robust, since MEA performance variation is not statistically significant as the manufacturing process parameters are varied. The best MEA performance observed in this DOE occurred with ultrasonic manufacturing energy flux of 9.0 J/mm^2 and a sealing pressure of 3.0 N/mm^2.

Real and reactive power versus time was measured for ultrasonic bonding of MEAs with optimal parameters (i.e., 9.0 J/mm^2 energy

flux or 9000 J and 3.0 N/mm^2 sealing pressure) using the setup described in Sec. 5 for thermal bonding. The average bonding cycle on the ultrasonic press requires 1.395 kW during operation. Multiplying the average power by time (7.7 second bonding cycle) yields an average energy consumption of 0.00298 kWh (0.0108 MJ) needed to thermally press one MEA.

7 Conclusions and Future Work

Ultrasonics has been shown to be a viable manufacturing process to bond components into low temperature PEM MEAs with significant energy and time savings over thermal bonding. Neither energy level nor sealing pressure, the two main process parameters identified, nor their interaction had a statistically significant effect on MEA performance suggesting that the process is very robust. However, electrode architecture and composition play an important role in the performance of ultrasonically bonded MEAs, since significant performance differences were observed over a small variety of electrodes.

With regards to thermal bonding, which involves orders-of-magnitude higher cycle time and energy usage, temperature is estimated to be a statistically significant effect whereas sealing pressure is not. Higher sealing temperatures resulted in thinner MEAs that showed better performance.

Comparing ultrasonics to thermal bonding in this particular case, cycle time (in seconds) for optimal process conditions is reduced by $(120 - 7.7)/120 = 93.6\%$. Likewise, energy consumption (in MJ) is reduced by $(0.648 - 0.0108)/0.648 = 98.3\%$.

Future work includes characterizing any differences in the losses between ultrasonic and thermal bonding. Quality of the ultrasonic bond and correlation to MEA performance for different GDE/membrane or GDL/CCM (catalyst coated membrane) material and architecture combinations may be characterized by simple lap shear or peel strength tests of MEAs. Optimized GDL may also improve any mass transport losses caused from the ultrasonic vibrations adversely affecting the electrode. This information can be used to intelligently design an electrode that is optimized for ultrasonic bonding. Current commercial electrodes are optimized for thermal bonding as that is the industry standard for production. Additional work plan includes scaling up the ultrasonic bonding process to MEAs with larger active areas and different membranes.

Acknowledgment

This research was supported by the U.S. Department of Energy through Grant #DE-FG36-08GO18053/A000).

References

[1] *The Fuel Cell Today Industry Review*, 2011, http://www.fuelcelltoday.com/media/1351623/industry_review_2011.pdf
[2] Snelson, T., Puffer, R., Pyzza, J., Walczyk, D., and Krishnan, L., 2011, "Method for the Production of an Electrochemical Cell," US and International patent pending.
[3] "Celtec®-P1000 MEA," 2012, BASF, Ludwigshafen, Germany, http://www.fuel-cell.basf.com/ca/internet/Fuel_Cell/en_GB/content/Microsite/Fuel_-Cell/Products/Celtec-P_1000
[4] Snelson, T., 2011, "Ultrasonic Sealing of PEM Fuel Cell Membrane Electrode Assemblies," Ph.D. thesis, Rensselaer Polytechnic Institute, Troy, NY.
[5] Krishnan, L., Snelson, T., Puffer, R., and Walczyk, D., 2010, "Durability Studies of PBI-Based Membrane Electrode Assemblies for High Temperature PEMFCs," Proceedings of the 6th Annual IEEE Conference on Automation Science and Engineering (CASE), Toronto, Canada, August 21–24, Paper No. 222.
[6] Share, D., Krishnan, L., Walczyk, D., Lesperence, D., and Puffer, R., 2010, "Thermal Sealing of Membrane Electrode Assemblies for High-Temperature PEM Fuel Cells," Proceedings of the ASME 8th International Fuel Cell Science, Engineering & Technology Conference, Brooklyn, NY, June 14–16, 2010, ASME Paper No. FuelCell2010-33227.
[7] Snelson, T., Pyzza, J., Krishnan, L., Walczyk, D., and Puffer, R., 2010, "Ultrasonic Sealing of Membrane Electrode Assemblies for High-Temperature PEM Fuel Cells," presented at the ASME 8th International Fuel Cell Science, Engineering & Technology Conference, Brooklyn, NY, June 14–16.
[8] "EC4019 Electrode EC4019," 2012, Fuel Cell Earth, Wakefield, MA, http://fuelcellearth.com/product/109-ec4019-electrode
[9] Hoffman, C., and Walczyk, D., 2011, "Direct Spraying of Catalyst Inks for PEMFC Electrode Manufacturing," Proceedings of the ASME 2011 Ninth International Fuel Science, Engineering and Technology Conference FuelCell2011, Washington DC, August 7–10, ASME Paper No. FuelCell2011-54416, pp. 911–917.
[10] "GDL 24 & 25 Series Gas Diffusion Layer," 2007, SGL Group, Wiesbaden, Germany, http://www.servovision.com/fuel_cell_components/gdl_24_25.pdf
[11] "DuPont Fuel Cells: DuPont™ Nafion® PFSA Membranes," 2009, DuPont Fuel Cells, Wilmington, DE, http://www2.dupont.com/FuelCells/en_US/assets/downloads/dfc101.pdf
[12] Gavach, C., Pamboutzoglou, G., Nedyalkov, M., and Pourcelly, G., 1989, "AC Impedance Investigation of the Kinetics of Ion Transport in Nafion Perfluorosulfonic Membranes," J. Membr. Sci., **45**, pp. 37–53.
[13] Zawodzinski, T., Derouin, C., Radzinski, S., Sherman, R., Smith, V., Springer, T., and Gottesfeld, S., 1993, "Water Uptake by and Through Nafion 117 Membranes," J. Electrochem. Soc., **140**(4), pp. 1041–1047.
[14] Gasteiger, H., Panels, J., and Yan, S., 2004, "Dependence of PEM Fuel Cell Performance on Catalyst Loading," J. Power Sources, **127**, pp. 162–171.
[15] Lee, W., Ho, C., Van Zee, J., and Murthy, M., "The Effects of Compression and Gas Diffusion Layers on the Performance of a PEM Fuel Cell," J. Power Sources, **84**, pp. 45–51.
[16] Liang, Z. X., Zhao, T. S., Xu, C., and Xu, J. B., 2007, "Microscopic Characterizations of Membrane Electrode Assemblies Prepared Under Different Hot-Pressing Conditions," J. Electrochim. Acta, **53**, pp. 894–902.
[17] Zhang, J., Yin, G. P., Wang, Z. B., Lai, Q. Z., and Cai, K. D., 2006, "Effects of Hot Pressing Conditions on the Performances of MEAs for DMFCs," J. Power Sources, pp. 73–81.
[18] "WattsOn™ - Universal Power Transducer," 2012, Elkor Technologies, Inc., London, Ontario, Canada, http://www.elkor.net/WattsOn.htm